OPEN ACCESS
Journal of Multidisciplinary Applied Natural Science Vol. xx No. xx (xxxx) https://doi.org/10.47352/jmans.2774-3047.461
Check for updates
Research Article

Mathematical Modeling and Cost-Effective Control of Tuberculosis through Vaccination and Treatment

Yudi Ari Adi*, Sugiyarto Sugiyarto, Desi Nurfita, Ummu Atiqah Mohd Roslan, and Suparman Suparman

Received : November 11, 2025	Revised : January 31, 2026	Accepted : May 26, 2026	Online : July 24, 2026

Abstract
Tuberculosis (TB) remains a major global health concern, particularly in high-burden countries such as Indonesia. To better understand the transmission dynamics and evaluate intervention strategies, a compartmental SVEITR model is developed that incorporates vaccination, exposure, treatment adherence, and immunity loss. Using next-generation matrix methods, the basic reproduction number (R_0) is derived and stability analysis demonstrated that the disease-free equilibrium is globally asymptotically stable when $R_0 < 1$. Bifurcation analysis of the vaccine efficacy parameter revealed a forward bifurcation, indicating that TB can be eradicated once vaccine efficacy exceeds a critical threshold. Using Pontryagin's maximum principle, we developed an optimal control problem with time-dependent vaccination and treatment adherence control. Numerical simulations demonstrated that the combined implementation of vaccination and treatment adherence resulted in the greatest reduction in the exposed and infectious population. Further cost-effectiveness analysis showed that improving treatment adherence alone was the most economically efficient strategy (ACER = 8.28; ICER = - 4.57), while vaccination alone was significantly less cost-effective (ACER = 297.67). Although combining vaccination with treatment adherence achieved additional health benefits, it incurs higher additional costs (ICER = 51.96). These findings suggest that treatment adherence should be prioritized in resource-limited settings, with combined strategies considered when additional resources are available.

Keywords: cost-effectiveness, forward bifurcation, optimal control, SVEITR model, Tuberculosis modeling

1. INTRODUCTION

Mathematical modeling plays a key role in understanding infectious disease dynamics and designing effective control strategies. Classic compartmental models such as the susceptible–infectious–recovered (SIR) model have provided a basic framework for describing transmission dynamics, threshold parameters, and long-term epidemic behavior. However, the reality of many infectious diseases involves complex latency periods, reinfections, and intervention strategies that cannot be adequately captured by basic SIR models. Tuberculosis (TB) presents unique modeling challenges due to its slow progression, latent infection stage, and partial immunity following treatment or vaccination [1]-[3]. To address these challenges, researchers have expanded the SIR framework by adding compartments for latency, reinfection, treatment, and vaccination. This expansion allows for the study of combined intervention programs, including preventive vaccination and case management through treatment [4]-[8].

A growing body of literature emphasizes that TB control requires a combination of strategies beyond vaccination alone. Combining vaccination with interventions to improve patient adherence and treatment completion can significantly reduce the critical vaccine efficacy needed to achieve disease elimination [9][10]. Even a moderately effective vaccine can substantially reduce TB incidence if supported by a strong adherence program and adequate treatment coverage. This finding is particularly relevant for high-burden countries like Indonesia, where treatment failure rates and delayed case detection remain major barriers to TB control [10].

Bifurcation analysis plays a crucial role in understanding how minor alterations in significant parameters can result in qualitative shifts in disease dynamics [11][12]. Identifying bifurcation thresholds helps policymakers target the most impactful parameters, for example, increasing treatment rates beyond a critical level or combining vaccination and treatment to shift the system toward a disease-free equilibrium. The theory of optimal

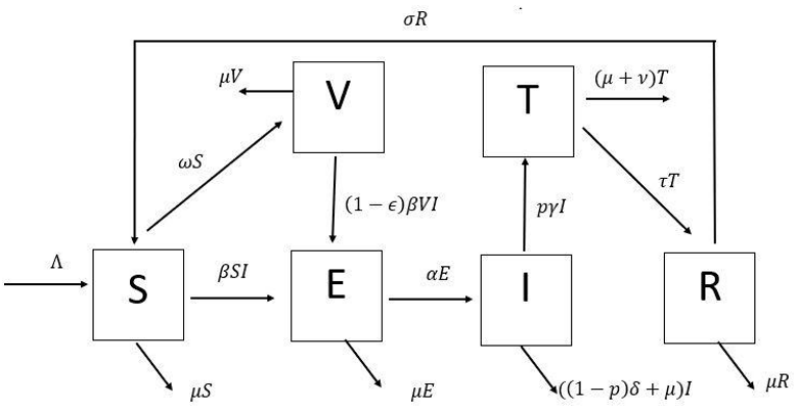

Figure 1. The flow diagram of the model.

control provides a formal framework for identifying cost-effective strategies to minimize TB prevalence and intervention costs. Recent studies have used an optimal control approach to determine the timing and intensity of vaccination and treatment strategies [9][13][14]. Cost-effectiveness analysis is crucial in this context, especially in resource-constrained regions, where public health budgets must be allocated efficiently [15][16].

Globally, TB remains one of the leading causes of infectious disease death, with 8.2 million new cases reported in 2023 according to the WHO Global TB Report 2024 [10]. Indonesia ranks among the two main contributors to the global TB incidence, accounting for approximately 10% of the global burden. Demographic factors, including a large working-age population and urban density, further complicate control efforts [17]. These challenges highlight the need for country-specific models that combine vaccination, treatment, adherence, and demographic data to inform local policy decisions. This study develops and analyzes the SVEITR model, an extension that includes key components of TB epidemiology: (i) vaccination as a preventive intervention, (ii) exposed individuals representing latent classes, (iii) treatment dynamics, including imperfect adherence and treatment saturation, and (iv) recovery with partial immunity. The model will then be calibrated with TB data from Indonesia. The model includes bifurcation analysis to identify threshold parameters and uses optimal control theory to determine the most cost-effective combination of vaccination and treatment interventions. By bridging mathematical analysis and practical public health considerations, this study provides actionable insights for TB control programs, supporting Indonesia's commitment to achieving the TB elimination target by 2030.

2. MATERIALS AND METHODS

2.1. Model Formulation

In this section, we construct a mathematical model that illustrates TB spread. We examine six distinct populations: $S(t)$ denotes susceptible individuals who have not been exposed to TB infection, $V(t)$ signifies vaccinated individuals against TB infection, $E(t)$ refers to individuals exposed to TB infection but who are not infectious, $I(t)$ represents diagnosed infectious individuals who have contracted TB, $T(t)$ indicates the class of individuals who get treatment, and $R(t)$ represents recovered individuals. The susceptible population increases due to a daily recruitment rate denoted as Λ, while susceptible individuals receive vaccination against TB infection at a constant rate of ω. We postulate that individuals vaccinated against TB infection lose their immunity after a certain period and may become infected following effective contact with infectious individuals at a diminished rate of 1 - ε. Consequently, the risk of infection for those who are vaccinated is expressed at the rate of $\beta(1 - \varepsilon)VI$.

We also assume that only individuals who are infected can transmit the infection; therefore, the risk of infection is expressed as βIS. The transition rate of individuals from the exposed class to the infectious class is denoted by α, while γ represents the progression rate from the infectious diagnosed to the treatment class. Individuals receiving treatment recover through hospital care at a rate of τ, and p indicates the level of patient adherence to

treatment. Treatment adherence is explicitly incorporated through the parameter p, which scales the recovery rate τ, so that higher adherence increases successful treatment outcomes, while lower adherence represents treatment interruption and failure. The parameter μ denotes the natural death rate across all compartments, and we assume that disease-induced mortality rate due to treatment failure occurs at rates δ, while additional mortality due to the disease occurs in T at a rate of v, with the condition that $\delta > v$. We assume the recovered individuals experience a loss of immunity at a rate σ and become susceptible again.

The proposed SVEITR model is developed based on several standard assumptions commonly adopted in tuberculosis transmission modeling. Recruitment into the susceptible population is assumed to occur at a constant rate, while natural mortality affects all compartments and disease-related mortality applies to both infected and treated individuals, implying that the total population size is not strictly constant. Homogeneous mixing is assumed, meaning all individuals have the same probability of contact, regardless of age or socioeconomic status. Age structure is not explicitly modeled. Instead, vaccination effects are captured through an effective vaccine parameter representing population -level protection rather than individual-level age stratification. These assumptions allow the model to capture important long-term transmission dynamics at the population level in Indonesia. However, age heterogeneity, socioeconomic disparities, and spatial variation can influence tuberculosis transmission and control outcomes. These aspects are therefore recognized as limitations of this study and important directions for future research. The above description is represented by the system of differential equations given in Equation (1), while the model compartment flow diagram is illustrated in Figure 1.

$$\begin{aligned}\frac{dS}{dt} &= \Lambda - \beta SI - \omega S + \sigma R - \mu S \quad \frac{dV}{dt} = \omega S - (1-\epsilon)\beta VI - \mu V \quad \frac{dE}{dt} \\ &= \beta SI + (1-\epsilon)\beta VI - (\alpha+\mu)E \quad \frac{dI}{dt} = \alpha E - (p\gamma + (1-p)\delta + \mu)I \quad \frac{dT}{dt} \\ &= p\gamma I - (\tau + \mu + v)T \quad \frac{dR}{dt} = \tau T - (\sigma + \mu)R\end{aligned} \tag{1}$$

with initial conditions:

$$S(0) \geq 0, \quad E(0) \geq 0, \quad V(0) \geq 0, \quad I(0) \geq 0, \quad T(0) \geq 0, \quad R(0) \geq 0. \tag{2}$$

It is important to highlight that all parameters utilized in the TB model are non-negative, as the model illustrates human population dynamics. Moreover, it is necessary to demonstrate that all six state variables of the proposed model remain non-negative at all times. We state in the theorem 1.

Theorem 1. Assume that all model parameters are non-negative, and $0 \leq \epsilon \leq 1$, $0 \leq p \leq 1$. Then the solutions of system (1) with the initial conditions (2) remain non-negative for every $t \geq 0$.

Proof. We apply the theory of positive

Table 1. Parameter values.

Parameter	Description	Value	Source
Λ	Recruitment rate	2,800,863	[19]
μ	Natural death rate	0.01381	[17]
β	Transmission rate of infected population	5,8178 x 10^{-9}	[19]
ε	Vaccine effectiveness	0.12	Assumed
ω	Vaccination rate	0.72	Assumed
α	Rate of progression from the exposed to infectious stage	0.16814	[19]
δ	Disease-induced death rate	0.02282	[20]
γ	Treatment rate	0.87	[20]
p	Level of patient adherence to treatment	0.5	Assumed
v	Disease mortality rate of treatment individuals	0.01	Assumed
σ	Lose immunity rate of recovered individuals	0.047634	[19]
τ	Recovery rate	0.645	[20]

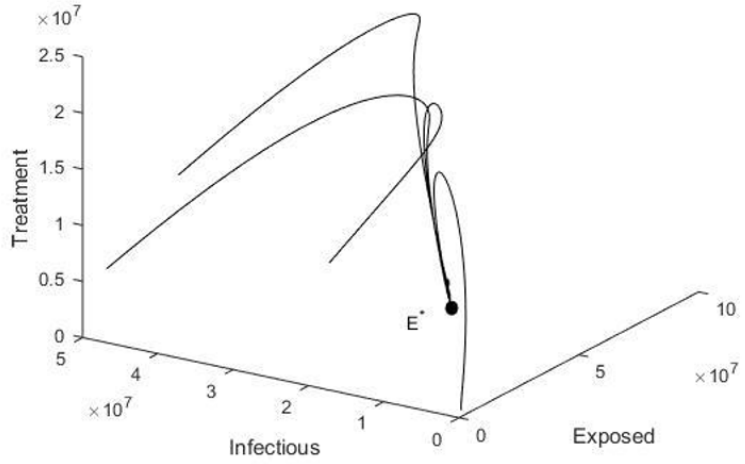

Figure 2. The phase portrait of the exposed, infected, and treatment population.

invariance. It suffices to verify that, at each boundary where a state variable becomes zero, the derivative of that variable is non-negative provided the other state variables are non-negative.

When $S = 0$, we have $\frac{dS}{dt} = \Lambda + \sigma R \geq 0$, when $V = 0$, $\frac{dV}{dt} = \omega S \geq 0$, when $E = 0$, $\frac{dE}{dt} = \beta SI + (1-\epsilon)\beta VI \geq 0$, when $I = 0$, $\frac{dI}{dt} = \alpha E \geq 0$, when $T = 0$, $\frac{dT}{dt} = p\gamma I \geq 0$, and when $R = 0$, $\frac{dR}{dt} = \tau T \geq 0$.

Hence, the vector field on the boundary of the non-negative orthant points inward or is tangent to the boundary. Due to the invariance of the non-negative orthant, every solution that starts with non-negative initial conditions will stay non-negative throughout all time. This completes the proof.

2.2. Equilibria and Basic Reproduction Number

System (1) always has a disease-free equilibrium point where no individuals are infected. Solving the linear steady-state equations gives the disease-free equilibrium (DFE) $E_0 = (S_0, V_0, 0, 0, 0, 0)$, whereas: $S_0 = \frac{\Lambda}{\omega + \mu}$, $V_0 = \frac{\omega\Lambda}{\mu(\omega+\mu)}$.

To determine the basic reproduction number of model (1), the widely used next-generation operator method and notation, which has been thoroughly examined previously [18], is utilized. Let $X = \{E, I\}$ represent the set of infected compartments. Consequently, the subsystem that outlines the dynamics of these compartments is derived from the TB model (1) and is expressed as follows:

$$\frac{dE}{dt} = \beta SI + (1-\epsilon)\beta VI - (\alpha+\mu)E \quad \frac{dI}{dt} = \alpha E - (p\gamma + (1-p)\delta + \mu)I$$

We find a new infection matrix as follows:

$$F = (\beta SI + (1-\epsilon)\beta VI\ 0), V = ((\alpha+\mu)E - \alpha E + (p\gamma + (1-p)\delta + \mu)I).$$

Linearize at the DFE, we get the matrices F and V:

$$F = \left(\beta\left(\frac{\Lambda}{\mu+\omega} + (1-\epsilon)\frac{\omega}{\mu}\cdot\frac{\Lambda}{\mu+\omega}\right) 0\ 0\ 0\right),\ V = (\alpha+\mu\ 0\ -\alpha\ p\gamma + (1-p)\delta + \mu).$$

One computes:

$$V^{-1} = \frac{1}{(\alpha+\mu)(p\gamma+(1-p)\delta+\mu)}(p\gamma + (1-p)\delta + \mu\ 0\ \alpha\ \alpha + \mu).$$

The next–generation matrix FV^{-1} is upper triangular, and its spectral radius equals its (1,1) entry:

$$R_0 = \rho(FV^{-1}) = \frac{\beta\alpha\Lambda}{(\mu+\omega)(\alpha+\mu)(p\gamma+(1-p)\delta+\mu)} \cdot \left(1 + \frac{(1-\epsilon)\omega}{\mu}\right). \quad \textbf{(3)}$$

2.3. Existence of an Endemic Equilibrium

The endemic equilibrium are solutions of $\dot{S} = 0$, $\dot{V} = 0$, $\dot{E} = 0$, $\dot{I} = 0$, $\dot{T} = 0$, $\dot{R} = 0$ denoted by $E^* = (S^*, V^*, E^*, I^*, T^*, R^*)$ where:

$$S^* = \frac{K((1-\epsilon)\beta I^* + \mu)}{(1-\epsilon)\beta I^* + \mu + (1-\epsilon)\omega}, \quad E^* = \frac{p\gamma + (1-p)\delta + \mu}{\alpha} I^*, \quad T^* = \frac{p\gamma}{\tau + \mu + \nu} I^*,$$

$$V^* = \frac{\omega}{(1-\epsilon)\beta I^* + \mu}\left(\frac{K((1-\epsilon)\beta I^* + \mu)}{(1-\epsilon)\beta I^* + \mu + (1-\epsilon)\omega}\right), \quad R^* = \frac{p\gamma\tau}{(\tau+\mu)(\sigma+\mu)} I^*.$$

With I^* is the positive real roots of:

$$A_2 I^2 + A_2 I + A_0 = 0, \quad \textbf{(4)}$$

where:

$A_2 = A(K\beta - \sigma c)$, $A_1 = AK(\omega + \mu) + K\mu\beta - \Lambda A - \sigma c(\mu + B)$, $A_0 = \Lambda(\mu + B)(1/R_0 - 1)$, **(5)**

and $A = (1-\epsilon)\beta, B = (1-\epsilon)\omega, K = \frac{(\alpha+\mu)(p\gamma+(1-p)\delta+\mu)}{\alpha\beta}$, and $c = \frac{p\gamma\tau}{(\tau+\mu)(\sigma+\mu)}$.

The theorem presented below articulates the existence of an endemic equilibrium.

Theorem 2. Consider the System (1). Let $\Phi = \frac{(\alpha+\mu)(p\gamma+(1-p)\delta+\mu)}{\alpha} - \sigma c$, R_0 be given by (3), and $\Delta = A_1^2 - 4A_2A_0$ with $\epsilon < 1$.

i. If $R_0 > 1$, then $A_0 < 0$ and hence (4) has exactly one positive real root. Consequently, (1) admits at least one endemic equilibrium with $I^* > 0$. Moreover, if $\Phi \neq 0$ the positive root is simple.
ii. If $R_0 < 1$ and either $\Phi \leq 0$ or $A_1 \geq 0$ or $\Delta \leq 0$, then (4) has no positive real root and (1) admits no endemic equilibrium.
iii. If $R_0 < 1$, $\Phi > 0$ (so $A_2 > 0$), $A_1 < 0$, and $\Delta > 0$, then (4) admits two distinct positive roots $0 < I_1^* < I_2^*$, hence (1) has two endemic equilibria.

Proof.

i. From (5), $A_0 = \Lambda(\mu + B)(1/R_0 - 1)$. Thus for $R_0 > 1$ we have $A_0 < 0$. Since $\epsilon < 1$ and $\beta > 0$, $A_2 = (1 - \epsilon)\beta\Phi$ is nonzero except on the nongeneric set $\Phi = 0$. Hence $A_0/A_2 < 0$, so (4) has exactly one positive and one negative real root. The positive root defines $I^* > 0$; back-substitution gives $S^*, V^*, E^*, T^*, R^* > 0$.
ii. For $R_0 < 1$ we have $A_0 > 0$. If either $A_2 \leq 0$ (i.e. $\Phi \leq 0$) or $A_1 \geq 0$ or $\Delta \leq 0$, then by Viète's relations $A_0/A_2 \leq 0$ or $-A_1/A_2 \leq 0$ or the roots are nonreal; in each case, no positive real root exists, so no endemic equilibrium.
iii. Suppose $R_0 < 1$ and $\Phi > 0$, hence $A_2 > 0$. If moreover $A_1 < 0$ then $-A_1/A_2 > 0$, and with $A_0 > 0$ we have $A_0/A_2 > 0$. Thus either both roots are positive or both negative. The discriminant condition $\Delta > 0$ guarantees the roots are real and unequal; combining with $-A_1/A_2 > 0$ yields two positive roots, hence two endemic equilibria.

The positivity of the remaining compartments follows from the linear relations given above and the non-negativity of parameters, once $I^* > 0$ is fixed.

Next, we show the stability of the disease-free equilibrium point in the theorem that follows.

Theorem 3. For the system (1), if $R_0 < 1$, then E_0 is locally asymptotically stable and if $R_0 > 1$, then E_0 is unstable.

Proof. By linearizing system (1), the Jacobian matrix at E_0 is obtained as

$J(E_0) = (-(\omega + \mu)\ 0\ 0\ -\beta S_0\ 0\ \sigma\omega\ -\mu\ 0\ -(1-\epsilon)\beta V_0\ 0\ 0\ 0\ 0\ -(\alpha+\mu)\ \beta S_0 + (1-\epsilon)\beta V_0\ 0\ 0\ 0\ 0\ \alpha\ -D\ 0\ 0\ 0\ 0\ 0\ p\gamma\ -(\tau+\mu+\nu)\ 0\ 0\ 0\ 0\ 0\ \tau\ -(\sigma+\mu)\ )$,

with $D := p\gamma + (1-p)\delta + \mu$.

The Jacobian matrix $J(E_0)$ has eigenvalues $-(\omega + \mu)$, $-\mu$, $-(\tau + \mu + \nu)$ and $-(\sigma + \mu)$, these are strictly negative. The other two eigenvalues are derived from the 2x2 matrix block $J_2 = (-(\alpha + \mu)\ \beta S_0 + (1 - \epsilon)\beta V_0\ \alpha\ -D)$.

The characteristic equation of J_2 is:

$\lambda^2 + (\alpha + \mu + D)\lambda + (\alpha + \mu)D(1 - R_0) = 0$,

which has negative roots if $R_0 < 1$ and has a positive roots if $R_0 > 1$. This proves that all

Table 2. Sensitivity index of each model parameters.

Parameter	Sensitivity index
Λ	1
β	1
γ	-0.9452
ω	-0.0108
μ	-1.0951
p	-0.9204
δ	-0.0248
α	0.0759
ε	-0.1230

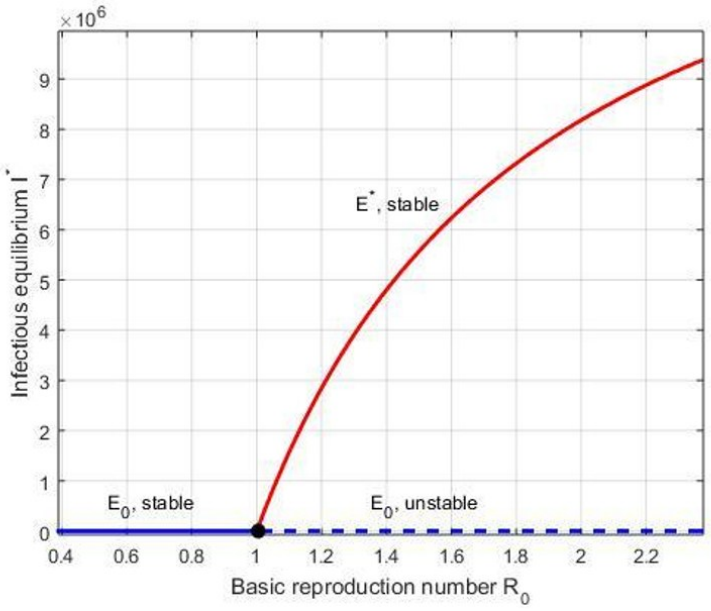

Figure 3. The continuation of the parameter ε reveals the occurrence of a forward bifurcation.

eigenvalues of $J(E_0)$ possess a negative real part if $R_0 < 1$, which proves local asymptotic stability of E_0. Conversely, if $R_0 > 1$ $J(E_0)$ exhibits a positive real eigenvalue, indicating that the DFE is unstable.

Theorem 4. If $R_0 \leq 1$ and $\Phi = \frac{(\alpha+\mu)D}{\alpha} - \sigma \frac{p\gamma\tau}{(\tau+\mu)(\sigma+\mu)} \leq 0$, then the disease–free equilibrium E_0 is globally asymptotically stable in the feasible region $\Omega = \{(S, V, E, I, T, R) \geq 0: S + V + E + I + T + R \leq \frac{\Lambda}{\mu}\}$.

Proof. Condition $\Phi = \frac{(\alpha+\mu)D}{\alpha} - \sigma \frac{p\gamma\tau}{(\tau+\mu)(\sigma+\mu)} \leq 0$ guarantees no positive root of the quadratic (4) when $R_0 < 1$. On this side, we will prove that the disease-free equilibrium is not only local but global. Define a linear Lyapunov function

$L(E,I) = aE + bI$

with positive constants a, b to be fixed. Differentiate along trajectories:

$$\dot{L} = \alpha(\beta(S + (1 - \epsilon)V)I - (\alpha + \mu)E) + b(\alpha E - DI)$$
$$= (\alpha\beta(S + (1 - \epsilon)V) - bD)I + (-a(\alpha + \mu) + b\alpha)E.$$

Choose $a = \frac{b\alpha}{\alpha+\mu}$ so that the coefficient of E vanishes. Then:

$$\dot{L} = b\left[\frac{\alpha}{\alpha+\mu}\beta(S + (1 - \epsilon)V) - D\right] I.$$

Since β scales linearly with R_0, one checks that for every t,

$$\frac{\alpha}{\alpha+\mu}\beta(S(t) + (1 - \epsilon)V(t)) - D \leq D(R_0 - 1).$$

Substituting into $\dot{L}$ gives:

$\dot{L} \leq b\, D\, (R_0 - 1)\, I$.

Therefore when $R_0 \leq 1$ we have $\dot{L} \leq 0$ on all Ω (and $\dot{L} = 0$ only when $I = 0$).

The set of possible states, denoted by Ω, is compact and positively invariant. The function L is always nonnegative and has a well-defined minimum in terms of the infected variables. According to LaSalle's invariance principle, every trajectory will eventually reach the largest subset of $\dot{L} = 0$. From the earlier analysis, when $\dot{L} = 0$, it means $I \equiv 0$. This leads to the conclusion that the exposed population $E \equiv 0$. We find that $T \rightarrow 0$, $R \rightarrow 0$. Meanwhile, the subsystem involving the susceptible and vaccinated populations (S,V) converges to (S_0,V_0). Therefore, every solution within Ω converges to the disease-free equilibrium E_0. This completes the proof.

Next, we prove the global stability of the endemic equilibrium point.

Theorem 5. The endemic equilibrium point $E^* = (S^*, V^*, E^*, I^*, T^*, R^*)$ of (1) is globally asymptotically stable when $R_0 > 1$.

Proof. Consider the Volterra–tycpe Lyapunov function

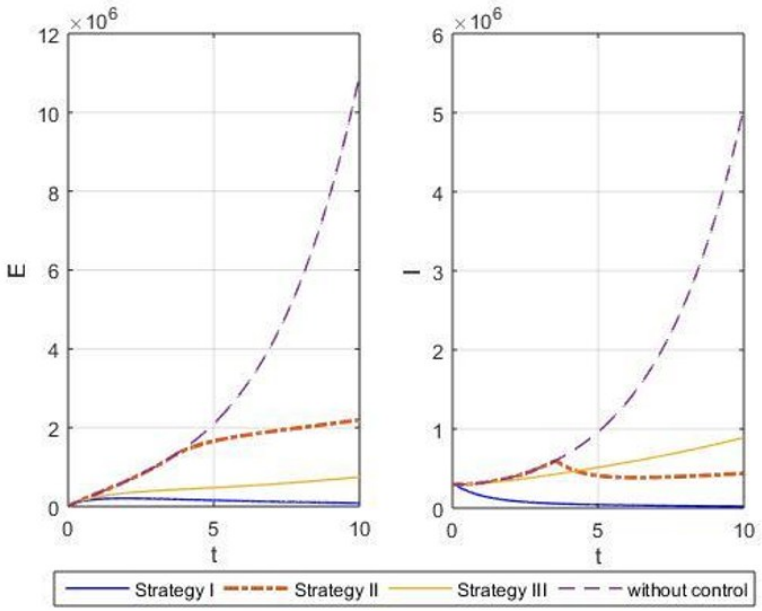

Figure 4. Simulation results with and without control strategies for the Exposed and Infected individuals.

$$V = \sum_{X\in\{S,V,E,I,T,R\}} a_X(X - X^* - X^* ln\frac{X}{X^*}),$$

with positive weights

$a_S = \beta I^*$, $a_V = (1 - \epsilon)\beta I^*$, $a_E = \alpha$, $a_I = D$, $a_T = \tau$, $a_R = \sigma$.

Each term $x - x^* - x^* ln(x/x^*)$ is nonnegative on R_6^+ and vanishes iff $x = x^*$. Differentiating along (1) at E^*,

$\beta S^* I^* + \omega S^* = (\sigma + \mu)R^* + \mu S^*$, $(1 - \epsilon)\beta V^* I^* + \mu V^* = \omega S^*$, $(\alpha + \mu)E^* = \beta I^* (S^* + (1 - \epsilon)V^*$, $DI^* = \alpha E^*$, $(\tau + \mu + \nu)T^* = p\gamma I^*$, $(\sigma + \mu)R^* = \tau T^*$,

we obtain after grouping terms:

$$\begin{aligned}\dot{V} &= -(\omega+\mu)\, a_S\, \Psi(\tfrac{S}{S^*}) - \mu\, a_V\, \Psi(\tfrac{V}{V^*}) - (\alpha+\mu)\, a_E\, \Psi(\tfrac{E}{E^*}) - D\, a_I\, \Psi(\tfrac{I}{I^*}) \\ &\quad -(\tau+\mu+\nu)\, a_T\, \Psi(\tfrac{T}{T^*}) - (\sigma+\mu)\, a_R\, \Psi(\tfrac{R}{R^*}), \\ &\le -C_1\, \Psi(\tfrac{S}{S^*}) - C_2\, \Psi(\tfrac{V}{V^*}) - C_3\, \Psi(\tfrac{E}{E^*}) - C_4\, \Psi(\tfrac{I}{I^*}) - C_5\, \Psi(\tfrac{T}{T^*}) - C_6\, \Psi(\tfrac{R}{R^*}),\end{aligned}$$

for some positive constants C_i depending on parameters and E^*, where $\Psi(u) = u - 1 - ln\ ln\ u$ 0. Hence $\dot{V} \le 0$ on Ω.

Since $\Psi(u) = 0$ iff $u = 1$, the largest invariant subset of $\{\dot{V} = 0\}$ is characterized by:

$$\frac{S}{S^*} = \frac{V}{V^*} = \frac{E}{E^*} = \frac{I}{I^*} = \frac{T}{T^*} = \frac{R}{R^*} = 1,$$

that is, the singleton E^*. Because solutions with $I(0) > 0$ remain in Ω, LaSalle's invariance principle implies $(S, V, E, I, T, R)(t)$ converges to E^*.

2.3. Bifurcation analysis

In a disease transmission model, the basic reproduction number, R_0 serves as a key threshold parameter for determining whether an infection can invade or persist within a population. The disease-free equilibrium is generally expected to be stable, implying that the disease will eventually die out if $R_0 \le 1$. However, under certain conditions, the system may exhibit more complex behavior, in which the relationship between R_0 and disease persistence is not straightforward. In this section, we will explore the bifurcation phenomenon associated with system (1). To examine the qualitative dynamics of the model, a bifurcation analysis is performed using the center manifold theorem.

The bifurcation analysis is performed with respect to the vaccine effectiveness parameter ε, which is selected as the primary bifurcation parameter to investigate qualitative changes in system behavior. By choosing ε as the bifurcation parameter, setting $R_0 = 1$ yields the following result:

$$\varepsilon = \varepsilon^* = 1 - \frac{\mu}{\omega}\left(\frac{1}{K} - 1\right), \quad \textbf{(6)}$$

with:

$$K = \frac{\beta\alpha\Lambda}{(\mu+\omega)(\alpha+\mu)(p\gamma + (1-p)\delta + \mu)}.$$

At the DFE $E_0 = (S_0, V_0, 0, 0, 0, 0)$, the Jacobian $J(E_0, \varepsilon^*)$ exhibits a simple zero eigenvalue at $\varepsilon = \varepsilon^*$, while all other eigenvalues are negative. Let $w = (w_1, w_2, \ldots, w_6)^T$ and $v = (v_1, v_2, \ldots, v_6)^T$ represent the corresponding right and left eigenvectors linked to the zero eigenvalues. Direct calculation, choosing the free scale $w_4 = 1$, yields the relationship.

$$w_3 = \frac{\beta S_0 + (1-\varepsilon^*)\beta V_0}{\alpha+\mu} w_4, \quad w_5 = \frac{p\gamma}{\tau+\nu+\mu} w_4, \quad w_6 = \frac{(1-p)\delta w_4 + \tau w_5}{\sigma+\mu},$$
$$w_1 = \frac{-\beta S_0 w_4 + \sigma w_6}{\omega+\mu}, \quad w_2 = \frac{\omega w_1 - (1-\varepsilon^*)\beta V_0 w_4}{\mu}.$$

Similarly, the left-eigenvector of the Jacobian matrix $J(E_0, \varepsilon^*)$ that fulfills the condition $v.w = 1$ is:

$$v = (0,0,\frac{\alpha}{\alpha+\mu},1,0,0)^\top,$$

so that, we have $v_E = v_3 = \alpha/(\alpha + \mu) > 0$.

Now, following Castillo-Chavez and Song [18], we calculate the coefficients a and b as follows:

$$a = \sum_{k,i,j=1}^{6} v_k w_i w_j \frac{\partial^2 f_k}{\partial x_i \partial x_j}(E_0, \varepsilon^*), \quad b = \sum_{k,i=1}^{6} v_k w_i \frac{\partial^2 f_k}{\partial x_i \partial \varepsilon}(E_0, \varepsilon^*),$$

Taking into account that the only nonzero second derivatives of the vector field come from the terms βSI and $(1 - \varepsilon)\beta VI$, then substitution of $v_1 = v_2 = 0$ and $v_3 = \frac{\alpha}{\alpha+\mu}$, we obtain:

$$a = \beta v_E(w_1 + (1 - \varepsilon^*)w_2), b_\varepsilon = -\beta V_0 v_E,$$

where $v_E = \frac{\alpha}{\alpha+\mu}$. For the unfolding $\eta = 1 - \varepsilon$ (which increases transmission as η grows) we have $b_\eta = -b_\varepsilon = \beta V_0 v_E > 0$.

According to the center-manifold theorem and traditional one-dimensional normal form analysis, when $\beta_\eta > 0$, the sign of a defines the type of bifurcation: $a > 0$ means a subcritical (backward) bifurcation, whereas $a < 0$ means a supercritical (forward) bifurcation. Substitute the expressions for w_6, w_1, w_2 (with $w_4 = 1$) into $a = \beta v_E(w_1 + (1 - \varepsilon^*)w_2)$, we get:

$$a = \beta v_E \frac{N}{\mu(\omega+\mu)Q_1},$$

Where $Q_1 = (\tau + \nu + \mu)(\alpha + \mu)$ and the numerator:

$N = (\sigma Q_2 - \beta S_0 Q_1)(\mu + (1 - \varepsilon^*)\omega) - (1 - \varepsilon^*)^2 \beta V_0 (\omega + \mu)Q_1$.

with $Q_2 = (1 - p)\delta(\tau + \nu + \mu) + \tau p\gamma$. Because $\beta > 0$, $v_E > 0$, and all denominator factors μ, $(\omega + \mu)$, Q_1 are strictly positive for admissible epidemiological parameters, hence $sign(a) = sign(N)$. Therefore the model admits a backward bifurcation at $\varepsilon = \varepsilon^*$ iff $N > 0$, and a forward bifurcation iff $N < 0$.

We have reached the following conclusion.

Theorem 6. System (1) at $R_0 = 1$, exhibits a backward bifurcation whenever the inequality $N > 0$ and a forward bifurcation whenever $N < 0$.

It should be noted that backward bifurcation only occurs if $A_2 > 0$, in which case the condition of Theorem 2(iii) is satisfied. If the condition of Theorem 2(iii) is not satisfied, then parameter continuation will indicate a forward bifurcation. Bifurcation analysis identifies critical thresholds in vaccine effectiveness that determine whether tuberculosis will persist or disappear, providing insight into the structural role of vaccination in disease elimination. Motivated by this threshold behavior, we next formulate an optimal control problem using time-dependent vaccination rate and treatment adherence controls to design practical intervention strategies that aim to drive the system toward a disease-free equilibrium in a cost-effective manner.

2.4. Optimal Control Problem for Vaccination and Treatment

We extend the system (1) to the optimal control problem. The optimal control problem is formulated by introducing time-dependent vaccination and treatment-adherence controls and minimizing an objective functional that balances the cumulative number of exposed and infectious individuals with the implementation costs of the control measures. Let $u_1(t)$ be the vaccination control rate varies with time and $u_2(t)$ the treatment control (per-capita treatment intensity for the fraction p that becomes treated). For $t \in [0, t_f]$ the corresponding state controlled system is:

$$\dot{S} = \Lambda - \beta SI - u_1(t)S + \sigma R - \mu S, \dot{V} = u_1(t)S - (1 - \epsilon)\beta VI - \mu V, \dot{E} = \beta SI + (1 - \epsilon)\beta VI - (\alpha + \mu)E, \dot{I} = \alpha E - (\gamma u_2(t) + (1 - \gamma)\delta + \mu)I, \dot{T} = \gamma u_2(t)I - (\tau + \mu + \nu)T, \dot{R} = \tau T - (\sigma + \mu)R, \quad (7)$$

with nonnegative initial state $x(0) = (S_0, V_0, E_0,$

I_0, T_0, R_0) ϵ Ω, where the feasible set is:

$$\Omega = \{x \geq 0: S + V + E + I + T + R \leq \Lambda / \mu\}.$$

We minimize the cost:

$$J(u_1,u_2) = \int_0^{tf}(A_1E(t) + A_2I(t) + \tfrac{1}{2} B_1u_1(t)^2 + \tfrac{1}{2} B_2u_2(t)^2)\, dt, \quad (8)$$

where A_1, $A_2 > 0$ are weight constants related to the epidemiological burden of E and I, and B_1, $B_2 > 0$ are the relative costs of implementing the controls. Here, the weighting coefficients represent the relative importance of reducing disease burden versus intervention costs. In other words, we want to find the best controls u_1* and u_2* that:

$$J(u_1^*,u_2^*) = \min_{u_1,u_2 \in U} J(u_1,u_2) \quad (9)$$

Where U is the set of admissible controls defined by:
$U = \{(u_1,u_2):u_i \epsilon L^{\infty}(0,t_f), 0 \leq u_1(t) \leq U_1, 0 \leq u_2(t) \leq U_2\}$,

With U_1,$U_2 > 0$ representing the maximum feasible effort for vaccination and treatment adherence.

Pontryagin's maximum principle is employed to derive the corresponding adjoint equations and characterize the optimal controls subject to bounded control constraints. To use Pontryagin's maximum principle, it is necessary to convert the system (7) and the objective functional (8) into a pointwise Hamiltonian, denoted as H, in relation to (u_1, u_2). This gives us

$$H = A_1E + A_2I + \tfrac{1}{2}B_1u_1^2 + \tfrac{1}{2}B_2u_2^2 + \lambda_S(\Lambda - \beta SI - u_1S + \sigma R - \mu S) + \lambda_V(u_1S - (1 - \epsilon)\beta VI - \mu V) + \lambda E(\beta SI + (1 - \epsilon)\beta VI - (\alpha + \mu)E) + \lambda_I(\alpha E - (\gamma u_2 + (1 - \gamma)\delta + \mu)I) + \lambda_T(\gamma u_2 I - (\tau + \mu + \nu)T) + \lambda_R(\tau T - (\sigma + \mu)R). \quad (10)$$

If (u_1*, u_2*, x*) is optimal then there exists absolutely continuous adjoint functions $\lambda(t) = (\lambda_S, \lambda_V, \lambda_E, \lambda_I, \lambda_T, \lambda_R)$ satisfying $-\dot{\lambda} = \nabla_x H$ a.e., with transversality conditions $\lambda_i(t_f) = 0$ for all i.

For the existence of optimal controls for model (7) alongside equation (9), we claim the optimal solution of system (7) in Theorem 7 below.

Theorem 7. There is an optimal control u_1*, u_2* that corresponds to the best solution (S*, V*, E*, I*, T*, R*) that minimizes the objective function (9) over U.

Proof. Taking the partial derivative of the Hamiltonian H with respect to the state variables gives us the adjoint system

$$-\dot{\lambda}_S = \lambda_S(-\beta I - u_1 - \mu) + \lambda_V u_1 + \lambda_E \beta I, -\dot{\lambda}_V = \lambda_V(-(1-\epsilon)\beta I - \mu) + \lambda_E(1-\epsilon)\beta I, -\dot{\lambda}_E = A_1 + \lambda_E(-\alpha - \mu) + \lambda_I \alpha, -\dot{\lambda}_I = A_2 - \lambda_S \beta S - \lambda_V(1-\epsilon)\beta V + \lambda_E(\beta S + (1-\epsilon)\beta V) + \lambda_I(-\gamma u_2 - (1-\gamma)\delta - \mu) + \lambda_T \gamma u_2, -\dot{\lambda}_T = \lambda_T(-\tau - \mu - \nu) + \lambda_R \tau, -\dot{\lambda}_R = \lambda_S \sigma + \lambda_R(-\sigma - \mu),$$

with $\lambda_i(t_f) = 0$.

Differentiating the Hamiltonian with respect to controls and imposing stationarity leads to the condition of optimal controls

$$\frac{\partial H}{\partial u_1} = B_1u_1 + (-\lambda_S + \lambda_V)S = 0, \frac{\partial H}{\partial u_2} = B_2u_2 + \gamma(-\lambda_I + \lambda_T)I = 0.$$

Thus, the pointwise optimal controls are

$$\hat{u}_1(t) = \frac{(\lambda_S(t) - \lambda_V(t))S(t)}{B_1}, \hat{u}_2(t) = \frac{\gamma(\lambda_I(t) - \lambda_T(t))I(t)}{B_2}.$$

Since $0 \leq u_i \leq U_i$, we get

$$u_1^*(t) = \Pi_{[0,U_1]}\left(\frac{(\lambda_S(t) - \lambda_V(t))\, S^*(t)}{B_1}\right), u_2^*(t) = \Pi_{[0,U_2]}\left(\frac{p(\lambda_I(t) - \lambda_T(t))\, I^*(t)}{B_2}\right),$$

where $\Pi_{[a,b]}(z) = min\{b, max\{a,z\}\}$. This completes the proof.

3. RESULTS AND DISCUSSIONS

To verify the analytical results presented in the

Table 3. Strategies I–III are arranged according to the ascending number of averted infections.

Strategy	Total cost (IDR)	Total cases averted	ACER	ICER
Without control	4.4163×10^8	0	-	-
Strategy II	4.5707×10^8	1.5355×10^6	297.67	10.054
Strategy III	2.8465×10^8	3.4386×10^7	8.2781	-4.5653
Strategy I	3.0882×10^8	3.4851×10^7	8.8613	-3.8106

previous section, we conducted numerical simulations of the SVEITR model. The first set of simulations focuses on the model without control, aiming to illustrate the stability properties of the equilibrium points and to visualize the bifurcation phenomena that occur when key parameters vary. The second set of simulations examines the model with optimal control, demonstrating the effects of implementing control strategies on the transmission dynamics of tuberculosis.

3.1. Numerical Results of the Model without Control Optimal

For the purpose of simulations, parameter values were obtained from previously published literature and Indonesian national data sources, rather than a complete parameter calibration performed in this study. Specifically, some epidemiological parameters were adopted from previous work [19], where the authors estimated model parameters using Indonesian tuberculosis data. Demographic parameters were obtained from Central Bureau of Statistics of Indonesia (BPS) [17], while tuberculosis-related parameters were informed by reports from the Indonesian Ministry of Health [20]. We note that national TB data may be affected by underreporting and delayed diagnosis; therefore, this analysis emphasizes qualitative dynamics rather than precise quantitative predictions. In the first numerical simulation, we verified the stability of the disease-free and endemic equilibrium points by examining the system trajectories at different initial conditions. This provides dynamic confirmation of the analytical stability criterion obtained through the basic reproduction number R_0. Secondly, we investigate the bifurcation behaviour of the system related to the reproduction number and vaccine efficacy parameters. In particular, we examine the occurrence of transcritical branching, where equilibrium stability reverses when R_0 exceeds one.

Meanwhile, BCG is highly effective against severe forms of TB in children when administered shortly after birth, with this protective effect potentially lasting up to ten years. However, its efficacy against pulmonary TB in adolescents and adults varies widely and generally declines over time [21]. Because the BCG vaccine is generally administered only to children and there is no revaccination program for adults, overall effectiveness is determined by a combination of the proportion of children in the population, the vaccination coverage rate and the vaccine effectiveness in children. Based on the census conducted by the Central Bureau of Statistics of Indonesia in 2022 [17], children under 10 years of age represent 16% of Indonesia's total population. Assuming a vaccine efficacy of 0.8, which covers 90% of children, this simulation selects vaccine effectiveness and vaccination rates of 0.12 and 0.72, respectively. These values are treated as illustrative baseline estimates reflecting current BCG coverage rather than precise population-wide measurements. The parameter values used in the simulation are summarized in Table 1. Robustness regarding vaccination assumptions is tested through bifurcation analysis of the vaccine efficacy parameter ε. This serves as the main branching parameter of the model, while β and ω remain fixed at their fundamental values. By varying ε over a biologically relevant range, we demonstrate forward bifurcation and identify a critical threshold at which tuberculosis elimination can be achieved. This suggests that the qualitative system dynamics and comparative effectiveness of intervention strategies are robust to fluctuations in vaccine efficacy.

By using the parameter values in Table 1, we obtain $R_0 = 2.0903 > 1$ so that the disease-free equilibrium point E_0 is unstable and there is only one endemic equilibrium point E^* which is globally asymptotically stable. Figure 2 demonstrates that, given the parameter values in Table 1, the phase portrait verifies the asymptotic stability of the endemic equilibrium. Biologically, irrespective of the initial size of any sub-population, tuberculosis will continue to persist within the society. To eliminate an endemic, the basic reproduction number R_0 must be reduced to below one. Mathematically, this can be achieved by varying the parameter values in the model. The parameters most suitable for intervention can be identified through sensitivity analysis, which evaluates how changes in each parameter influence the value of R_0.

The sensitivity index R_0 for each model parameter are presented in Table 2. Although the sensitivity index β (the transmission rate of the infected population) is equal to one, indicating the highest sensitivity, we did not focus on variations in this parameter in our analysis. This is because

Table 4. Comparison between strategies I and III.

Strategy	Total cost (IDR)	Total cases averted	ICER
Strategy III	2.8465×10^{8}	3.4386×10^{7}	8.2781
Strategy I	3.0882×10^{8}	3.4851×10^{7}	51.961

modifying the transmission rate has been extensively explored in previous studies and, in practice, requires stringent behavioral or social interventions that are difficult to maintain. Similarly, the parameters recruitment rate (Λ) and the natural death rate (μ) also exhibit high sensitivity indices. However, it is not realistic to manipulate these values, since they are intrinsic demographic factors beyond the scope of public health interventions. Furthermore, there are also parameters with high sensitivity indices, namely treatment rate (γ) and patient adherence to therapy (p). However, even when these parameters are increased to their maximum value (-1), the basic reproduction number (R_0) remains greater than one. This suggests that relying solely on transmission reduction or treatment-based interventions will still be insufficient to eliminate TB. Therefore, in our simulations, we focused on variations in the vaccine effectiveness parameter (ε) to investigate its impact on system dynamics, particularly changes in R_0 and the occurrence of bifurcation.

Continuation of the parameter ε, using the parameter values in Table 1, yields a bifurcation coefficient of $N = -11.39109 < 0$. According to Theorem 6, the bifurcation that occurs is a forward (supercritical) bifurcation. This result implies that as ε passes its critical value, the system transitions smoothly from an endemic to a disease-free state, and the endemic equilibrium disappears for higher values of ε. Biologically, this implies that increasing vaccine effectiveness above a critical threshold can stabilize the disease-free equilibrium, while also providing theoretical support for an effective strategy for disease elimination by intensifying vaccination efforts. Figure 3 shows the occurrence of a forward bifurcation at $R_0 = 1$, corresponding to a critical vaccine effectiveness of $\varepsilon = 0.58901$. This finding emphasizes that achieving disease elimination requires a sufficiently high level of vaccine effectiveness. These results also strengthen the argument that tuberculosis vaccination programs should not be limited to children. Because adults also play a critical role in the dynamics of disease transmission, the development and implementation of an effective TB vaccine for the adult population is crucial. Therefore, research efforts and public health initiatives that aim to discover, improve and distribute a TB vaccine for adults need to be further intensified to ensure long-term control and eventual eradication of this disease.

3.2. Numerical Results of the Model with Control Optimal

We used the forward-backward sweep technique as described previously [22], which is very common in the literature on optimal control problems, to find the optimal trajectories of the optimal system. We set $U_1 = 0.9$ for control with vaccination, assuming that the vaccine is not yet fully effective and people are less aware of the need for vaccination, and $U_2 = 0.9$ for maximum control, assuming that it is hard to get people to stick to their medication. We will focus on comparing the three control strategies.

i. Strategy I: Combination of vaccination and treatment. Here, u_1 and u_2 are set as control variables.
ii. Strategy II: Vaccine intervention as the only control. In this case, only u_1 is taken as the control variable.
iii. Strategy III: Use medication adherence as a control, so only u_2 is the control variable.

To study the dynamics of exposed, E and infected populations, I, numerical simulations were performed using four scenarios: (i) without control, (ii) strategy I (two controls u_1 and u_2 applied simultaneously), (iii) strategy II (only u_1), and (iv) strategy III (only u_2). Figure 4 shows that the without control scenario leads to an increase in the number of individuals in compartments E and I over time, indicating uncontrolled disease spread. Meanwhile, the simultaneous implementation of

strategy I (two controls) results in a significant decrease in the number of individuals in compartments E and I. The curves for E and I decrease more rapidly and stabilize near zero by the end of the simulation period, indicating that the combination of vaccination and treatment is effective in suppressing transmission and accelerating population recovery. Implementation of strategy II (controlling only u_1) also shows a decrease in the number of cases of E and I compared to without control, although not as optimal as strategy I. Strategy III (controlling only u_2) has the smallest impact in reducing E and I. The graph shows a relatively slow decrease in cases, especially in the compartment I, indicating that treatment alone is insufficient to control the outbreak in the considered time period. These results suggest that the simultaneous use of two control strategies yields the most effective results in reducing the number of individuals exposed and infected compared to using a single control strategy alone.

3.3. Cost-effectiveness Analysis

Following previous studies on disease modeling and optimal intervention design [15][23]-[25] a cost -effectiveness analysis (CEA) was performed to assess the economic implications of the proposed control strategies. The cost-effectiveness of each control strategy was evaluated using four quantitative indicators: total cost, total cases averted, the average cost-effectiveness ratio (ACER), and the incremental cost-effectiveness ratio (ICER). The total cost associated with a given control strategy (u_1,u_2) is defined in Equation (11):

$$T_C = \int_0^{tf} (c_1\, u_1(t)\, S(t) + c_2\, u_2(t)\, I(t))\, dt, \quad \textbf{(11)}$$

Where c_1 and c_2 represent the unit costs of vaccination and treatment, respectively. The total number of cases averted, which measures the epidemiological effectiveness of the intervention, is given by Equation (12):

$$T_C = \int_0^{tf} (I_0(t) - I_{u1,u2}(t))\, dt, \quad \textbf{(12)}$$

Where $I_0(t)$ and $I_{u1,u2}(t)$ denote the infected populations in the absence and presence of controls, respectively. The ACER quantifies the average cost per case averted and is computed as below.

$$ACER = \frac{T_C}{T_A}. \quad \textbf{(13)}$$

To compare alternative strategies, the ICER is employed, defined as:

$$ICER_{i,j} = \frac{C_j - C_i}{A_j - A_i}, \quad \textbf{(14)}$$

which expresses the additional cost required to avert one additional case when moving from strategy i to strategy j. A negative ICER value indicates that the new strategy is dominant, meaning it is both more effective and less costly than the alternative.

Using Equations (11)–(14), the results of the cost -effectiveness analysis are summarized in Table 3. In this study, the cost of vaccination per individual was assumed to be IDR 150,000, and the cost of care per infected individual was set at IDR 365,000 per person per year. Due to the lack of officially published per-unit cost data for TB vaccination and treatment at the national level, the authors assumed the costs of vaccination (IDR 150,000 per individual) and treatment (IDR 365,000 per patient per year) as representative baseline values within commonly reported ranges. These values are intended to provide illustrative estimates of comparative cost-effectiveness rather than precise economic evaluations. Based on Table 3, the total cost for the without-control scenario was IDR 4.4163 x 10^8, representing the total health burden attributable to exposed, E and infected, I individuals. Implementation of strategy II (vaccination only) increased the total cost to IDR 4.5707 x 10^8, indicating that vaccination as a stand-alone intervention resulted in higher expenditures with only modest health benefits. Conversely, strategy III (improved treatment adherence) significantly reduced the total cost to IDR 2.8465 x 10^8, indicating that improved treatment adherence not only reduced the disease burden but also generated relatively substantial cost savings. Combined control (strategy I, vaccination plus adherence to treatment) also resulted in cost savings compared to baseline (IDR 3.0882 x 10^8), although cost savings were slightly lower than those of strategy III alone. In terms of prevented cases, strategy II prevented approximately 1.5355 x 10^6

cases, while strategy III prevented approximately 3.4386×10^7 cases, more than twenty times more effective than vaccination alone. Combining these two interventions further improved health outcomes by preventing an additional 4.65×10^5 cases compared to strategy III, but at a significantly higher cost.

The ACER highlights this difference in efficiency. Strategy II required 297.67 cost units per case prevented, which is relatively inefficient compared to Strategy III's 8.2781 cost units per case prevented. The combined strategy had an ACER of 8.8613, slightly less efficient than strategy III alone, reflecting the diminishing returns of adding vaccination to an already effective treatment program. The ICER confirmed these findings. Strategy II had a positive ICER (10.054), indicating that it was more expensive and only slightly more effective than the baseline strategy. In contrast, strategy III has a negative ICER (-4.5653), indicating that it is dominant, being simultaneously more effective (more cases prevented) and less costly than no intervention. Strategy I also demonstrates dominance over the baseline (-3.8106), but its cost savings are lower compared to strategy III. Pairwise comparisons show that strategy III strictly dominates strategy II, as the shift from vaccination to treatment adherence simultaneously reduces costs and prevents more cases. Consequently, strategy II was eliminated from the list of potential control strategies. The ICERs for strategies III and I were then recalculated, and the results are presented in Table 4. Adding vaccination to strategy III, thus becoming strategy I, provided only marginal additional health benefits at a significantly higher cost, resulting in an ICER of 51.961 per case prevented.

These results indicate that increasing treatment adherence (strategy III) is the most cost-effective intervention, providing the most significant decrease in disease burden at the lowest cost. The integration of vaccination with treatment adherence can be considered if sufficient resources are available and decision-makers are willing to pay for the additional benefits, but vaccination alone is not recommended because it is neither cost-saving nor highly effective.

To evaluate the robustness of the cost-effectiveness results, a simple sensitivity analysis was conducted by varying the costs of vaccination and treatment. We considered two scenarios. Scenario 1 increased vaccination costs by 50%, while treatment costs were reduced by 25%. In scenario 2, vaccination costs were reduced by 25%, while treatment costs were increased by 50%. The results of this analysis are summarized in Table 5. It can be observed that strategy III consistently produced negative ICER values across all scenarios. This indicates that strategy III remains dominant, meaning it is both cheaper and more effective than the alternative strategies. Although strategy I also produced negative ICER values, it incurs higher costs, but the number of cases prevented did not increase significantly compared to strategy III. Therefore, this strategy can be considered weakly dominated. Meanwhile, strategy I showed relatively high ICER values across all scenarios, indicating that it is not cost-effective. These results indicate that strategy III's dominance remains across all tested scenarios, thus strengthening the reliability of the policy recommendation.

4. CONCLUSIONS

This study develops and analyses the SVEITR model to investigate the dynamics of tuberculosis transmission in Indonesia and evaluate cost-effective intervention strategies. This analysis shows that the global disease-free equilibrium is asymptotically stable when the basic reproduction

Table 5. Sensitivity analysis of ICER under different cost scenarios.

Strategy	ICER			Interpretation
	Baseline	Scenario 1	Scenario 2	
Strategy II	10.054	20.2380	4.9627	Not cost-effective
Strategy III	-4.5653	-4.9999	-3.6962	Dominant
Strategy I	-3.8106	-3.7751	-3.1999	Weakly dominated

number $R_0 < 1$. Bifurcation analysis of vaccine efficacy shows a forward bifurcation, suggesting that tuberculosis elimination can be achieved without bistability when vaccine efficacy exceeds a critical threshold. This means that a sufficiently strong vaccination effort can reliably eliminate the disease regardless of initial conditions. Optimal control analysis shows that time-dependent interventions in vaccination and compliance can effectively reduce exposure and infected populations. Numerical simulations show that a combination of vaccination and compliance accelerates the approach to disease-free equilibrium and has the greatest epidemiological impact. These results are consistent with theoretical bifurcation analysis, where strong combined interventions shift the system into the $R_0 < 1$ region. From an economic perspective, cost-benefit analysis provides clear policy-relevant insights. Based on the assumed unit cost values, increased compliance alone was found to be the most economically efficient strategy, with a low average cost-effectiveness ratio (ACER = 8.28) and a negative incremental cost-effectiveness ratio (ICER = -4.57), indicating superiority over the no-control scenario. Vaccination as a single intervention was significantly less cost-effective (ACER = 297.67). The combination of vaccination and compliance further reduced the burden of TB, but resulted in significantly higher additional costs (ICER = 51.96 per additional case prevented). These results suggest that in resource-limited settings, prioritizing treatment adherence has the greatest impact on health per unit cost, whereas combination strategies may be justified when additional resources are available and higher willingness-to-pay thresholds are acceptable. Several limitations of this study should be acknowledged. The model assumes homogeneous mixing and does not explicitly incorporate age structure or socioeconomic heterogeneity, which may affect tuberculosis transmission dynamics and intervention effectiveness. Furthermore, uncertainty in the assumed cost parameters and epidemiological estimates may influence the quantitative results. Future research should expand the model to include populations stratified by age, spatial or socioeconomic structure, and more accurate cost data to further enhance its relevance for national tuberculosis control policy.

AUTHOR INFORMATION

Corresponding Author

Yudi Ari Adi — Department of Mathematics, Universitas Ahmad Dahlan, Yogyakarta-55191 (Indonesia);
orcid.org/0000-0002-1831-9103
Email: yudi.adi@math.uad.ac.id

Authors

Sugiyarto Sugiyarto — Department of Mathematics, Universitas Ahmad Dahlan, Yogyakarta-55191 (Indonesia);
orcid.org/0000-0001-6210-7258

Desi Nurfita — Department of Public Health Sciences, Universitas Ahmad Dahlan, Yogyakarta-55164 (Indonesia);
orcid.org/0009-0003-0783-8754

Ummu Atiqah Mohd Roslan — Special Interest Group Modelling and Data Analytics, Universiti Malaysia Terengganu, Terengganu-21030 (Malaysia);
orcid.org/0000-0002-4396-0947

Suparman Suparman — Department of Mathematics Education, Universitas Ahmad Dahlan, Yogyakarta-55191 (Indonesia);
orcid.org/0000-0001-5526-6285

Author Contributions

Conceptualization, Y. A. A. and S. G.; Methodology, Software, and Formal Analysis, Y. A. A., S. G. and U. A. M. R.; Validation and Data Curation, D. N., S. P., and U. A. M. R.; Resources and Funding Acquisition, Y. A. A.; Investigation and Writing – Original Draft Preparation, Y. A. A., S. G., S. P., U. A. M. R.; Writing – Review & Editing, Y. A. A., D. N., and S. G.; Visualization, Y. A. A., U. A. M. R.; Project Administration, S. G., D. N.

Conflicts of Interest

The authors declare no conflict of interest.

ACKNOWLEDGEMENT

This research is supported by Directorate of

Research and Community Service, Ministry of Higher Education, Science and Technology of Indonesia, under the Fundamental Research Grant Scheme with a contract number of 126/C3/DT.05.00/PL/2025, 0498.12/LL5-INT/AL.04/2025, and 133/PFR/LPPM. UAD/V/2025.

DECLARATION OF GENERATIVE AI

During the preparation of this work the author(s) used *ChatGPT (OpenAI)* in order to improve the clarity and language of the manuscript. After using this tool/service, the author(s) reviewed and edited the content as needed and take(s) full responsibility for the content of the publication.

REFERENCES

[1] A. O. Egonmwan and D. Okuonghae. (2019). "Mathematical Analysis of a Tuberculosis Model with Imperfect Vaccine". *International Journal of Biomathematics*. **12** (7): 1950073. 10.1142/S1793524519500736

[2] L. N. Nkamba, T. T. Manga, F. Agouanet, and L. Nkague. (2019). "Mathematical Model to Assess Vaccination and Effective Contact Rate Impact in the Spread of Tuberculosis". *Journal of Biological Dynamics*. **13** (1): 26–42. 10.1080/17513758.2018.1563218.

[3] K. Das, B. S. N. Murthy, S. Abdus, and H. Ali. (2021). "Mathematical Transmission Analysis of SEIR Tuberculosis Disease Model". *Sensors International*. **2** : 100120. 10.1016/j.sintl.2021.100120.

[4] F. Sulayman and F. A. Abdullah. (2021). "An SVEIRE Model of Tuberculosis to Assess the Effect of an Imperfect Vaccine and Other Exogenous Factors". *Mathematics*. **9** (4): 327. 10.3390/math9040327.

[5] M. M. Ojo and E. F. Doungmo Goufo. (2023). "The Impact of COVID-19 on a Malaria Dominated Region: A Mathematical Analysis and Simulations". *Alexandria Engineering Journal*. **65** : 23–39. 10.1016/j.aej.2022.09.045.

[6] T. T. Yusuf and A. Abidemi. (2023). "Healthcare Analytics: Effective Strategies Towards Eradicating the Tuberculosis Epidemic: An Optimal Control Theory Alternative". *Healthcare Analytics*. **3** : 100131. 10.1016/j.health.2022.100131.

[7] O. James, D. Aldila, T. Abosede, G. Bolanle, and F. Abiodun. (2025). "Modeling Tuberculosis Dynamics with Vaccination and Treatment Strategies". *Scientific African*. **28** : e02647. 10.1016/j.sciaf.2025.e02647.

[8] V. M. Mbalilo, F. Nyabadza, and S. P. Gatyeni. (2025). "Modelling the Potential Impact of TB-Funded Prevention Programs on the Transmission Dynamics of TB". *Infectious Disease Modelling*. **10** (4): 1037–1054. 10.1016/j.idm.2025.05.010.

[9] T. Kang, H. Huo, and H. Xiang. (2024). "Dynamics and Optimal Control of Tuberculosis Model with the Combined Effects of Vaccination, Treatment and Contaminated Environments". *Mathematical Biosciences and Engineering*. **21** : 5308–5334. 10.3934/mbe.2024234.

[10] F. Pennisi, S. Borlini, R. Cuciniello, A. C. D'Amelio, R. Calabretta, A. Pinto, and C. Signorelli. (2025). "Improving Vaccine Coverage Among Older Adults and High-Risk Patients: A Systematic Review and Meta-Analysis of Hospital-Based Strategies". *Healthcare (Basel)*. **13** (14): 10.3390/healthcare13141667.

[11] M. Aguiar, V. Steindorf, A. K. Srivastav, N. Stollenwerk, and B. W. Kooi. (2024). "Bifurcation Analysis of a Two Infection SIR -SIR Epidemic Model with Temporary Immunity and Disease Enhancement". *Nonlinear Dynamics*. **112** : 13621–13639. 10.1007/s11071-024-09710-9.

[12] C. Guo and P. Wu. (2026). "Dynamics and Optimal Control for Tuberculosis Transmission via a Data-Validated Periodic Model". *Infectious Disease Modelling*. **11** (1): 121–142. 10.1016/j.idm.2025.09.002.

[13] I. Law and K. Floyd. (2020). "National Tuberculosis Prevalence Surveys in Africa, 2008–2016: An Overview of Results and Lessons Learned". *Tropical Medicine & International Health*. **25** (11): 1308–1327. 10.1111/tmi.13485.

[14] H. Fu, J. A. Lewnard, I. Frost, R. Laxminarayan, and N. Arinaminpathy. (2021). "Modelling the Global Burden of

Drug-Resistant Tuberculosis Avertable by a Post-Exposure Vaccine". *Nature Communications*. **12** (1): 424. 10.1038/s41467-020-20731-x.

[15] D. B. Kitaro, B. K. Bole, and K. P. Rao. (2024). "Optimal Control Strategies and Cost -Effectiveness Analysis of Tuberculosis Dynamics with Multidrug-Resistant Compartment". *Discrete Dynamics in Nature and Society*. 7235040. 10.1155/2024/7235040.

[16] Y. A. Adi, N. Irsalinda, and M. Z. Ndii. (2022). "Optimal Control and Cost-Effectiveness Analysis in an Epidemic Model with Viral Mutation and Vaccine Intervention". *CAUCHY: Jurnal Matematika Murni dan Aplikasi*. **7** (2): 173–185. 10.18860/ca.v7i2.13184.

[17] S. Suyatno, W. Lilis, and L. H. Izdihar. (2026). "The Determinants of Stunting Among Children Under Five In Central Java Based On Indonesian Nutritional Status Survey 2022". *Media Gizi Indonesia.* **21** (2): 247-262. 10.20473/mgi.v21i2.247-262.

[18] C. Castillo-Chavez and B. Song. (2004). "Dynamical Models of Tuberculosis and Their Applications". *Mathematical Biosciences and Engineering*. **1** : 361–404. 10.3934/mbe.2004.1.361.

[19] Y. A. Adi and Suparman. (2024). "An Investigation of Susceptible-Exposed-Infectious-Recovered (SEIR) Tuberculosis Model Dynamics with Pseudo-Recovery and Psychological Effect". *Healthcare Analytics*. 6 : 100361. 10.1016/j.health.2024.100361.

[20] A. M. I. Saktiawati and A. Probandari. (2025). "Tuberculosis in Indonesia: challenges and future directions". *The Lancet Respiratory Medicine.* **13** (8): 669-671. 10.1016/S2213-2600(25)00168-7.

[21] R. Lai, A. F. Ogunsola, T. Rakib, and S. M. Behar. (2023). "Key Advances in Vaccine Development for Tuberculosis: Success and Challenges". *NPJ Vaccines*. **8** (1): 158. 10.1038/s41541-023-00750-7.

[22] S. Lenhart and J. T. Workman. (2007). "Optimal Control Applied to Biological Models". Chapman & Hall/CRC. 10.1201/9781420011418.

[23] Z. Chazuka, C. E. Madubueze, and D. Mathebula. (2024). "Modelling and Analysis of an HIV Model with Control Strategies". *Results in Control and Optimization*. **14** : 100355. 10.1016/j.rico.2023.100355.

[24] A. Kuddus, A. K. Paul, and T. Theparod. (2024). "Cost-Effectiveness Analysis of COVID-19 Intervention Policies Using a Mathematical Model: An Optimal Control Approach". *Scientific Reports*. **14** : 1–19. 10.1038/s41598-023-50799-6.

[25] M. Z. Ndii and Y. A. Adi. (2021). "Understanding the Effects of Individual Awareness and Vector Controls on Malaria Transmission Dynamics Using Multiple Optimal Control". *Chaos, Solitons & Fractals*. **153** : 111476. 10.1016/j.chaos.2021.111476.